Design of a 4-level active photonics phase change switch using VO_2 and $Ge_2Sb_2Te_5$

Yun Meng,[1,2,3] Jitendra K. Behera,[1] Yujie Ke,[4] Litian Chew,[1] Yang Wang,[2] Yi Long,[4,a)] and Robert E. Simpson[1,a)]
[1]*ACTA Lab, Singapore University of Technology and Design, 8 Somapah Road, 487372 Singapore*
[2]*Key Laboratory of High Power Laser Materials, Shanghai Institute of Optics and Fine Mechanics, Chinese Academy of Sciences, Shanghai 201800, China*
[3]*University of Chinese Academic of Science, Beijing 10080, China*
[4]*School of Materials Science and Engineering, Nanyang Technological University, 50 Nanyang Avenue, Singapore 639798, Singapore*

(Received 10 June 2018; accepted 23 July 2018; published online 13 August 2018)

The objective of this work is to design and demonstrate multilevel optical switches by combining different phase change materials. $Ge_2Sb_2Te_5$ and VO_2 nanolayer structures were designed to maximize the optical contrast between four different reflective states. These different optical states arise due to the independent structural phase transitions of VO_2 and $Ge_2Sb_2Te_5$ at different temperatures. The transfer matrix method was used to model Fresnel reflection for each structural phase combination and then to optimize the VO_2 and $Ge_2Sb_2Te_5$ layer thicknesses, which were found to be 70 nm and 50 nm. These multilevel optical switching results provide further possibilities to design composite materials for applications in active and programmable photonics. *Published by AIP Publishing.* https://doi.org/10.1063/1.5043521

In recent decades, active photonics has attracted considerable attention for all-photonic multilevel-memory, holographic displays, and radiative homeostasis and for providing the necessary non-linearity for photonic artificial neural networks.[1–4] Phase change materials (PCMs) are now being studied and applied to tune these photonic devices.[5–14] PCMs exhibit a large change to their dielectric constant upon a structural transition.[15] Thus, PCMs can be incorporated into photonic structures to make them tunable. Heat, which is usually supplied by an electric current or a laser pulse, is used to trigger a reversible phase transition between two structural states.[16,17] In particular, the well-known phase change alloy $Ge_2Sb_2Te_5$ (GST) is attractive for applications in nano-photonics due to its excellent scaling[18,19] and fast structural transitions.[20] Vanadium dioxide (VO_2) is also a phase change material that exhibits a structural transformation and concomitant change to its electrical and optical properties at 68 °C.[21] VO_2 has been widely explored for energy storage[22,23] and switchable devices.[24–26]

Analogue optical tuning of the refractive index is highly desirable for active photonics. However, it is difficult to do this with individual layers of VO_2 and GST, as both exhibit abrupt transitions over a narrow temperature range, i.e., each material is either "on" or "off." This limits their application in multilevel devices. To solve this problem, we previously explored CSb_2Te_3, which progressively crystallizes over a large temperature range.[27] However, short laser pulses are required to transform the material to a specific optical state. Therefore, we now explore how VO_2 and GST can be combined to form a 2-bit, 4-state optical switch. We hypothesize that the different transition temperatures of VO_2 and GST will provide the possibility to achieve multilevel optical states.

We designed and experimentally demonstrated a prototype multilevel optical switch based on VO_2 and GST. We maximized the optical contrast by optimizing the layer order and thickness using the transfer matrix approach.[28] By comparing the reflectivity of different layer designs, we found that the optimized nanostructure layer order is SiO_2/VO_2/GST/Al. We grew this prototype structure and measured its reflectivity as a function of temperature. Four different reflectivity states were achieved with a total reflectivity change of 44% in the visible spectrum. Finally, the measurements and models were compared and validated with the predicted simulation results.

To calculate the optical reflectivity of the nanostructure, the dielectric-constants of VO_2 and GST films are required. The optical constants were measured by Variable Angle Spectroscopic Ellipsometry (VASE) using a Woollam M2000 ellipsometer. A Drude-Lorentz model[29] was used to fit the experimental data and the optical constants n and k were calculated. The fitted refractive index, n, and extinction coefficient, k, of GST and VO_2 films are shown in Fig. 1. For further details, see Ref. 30. Figure 1(a) shows that there is a substantial change in the refractive index of the VO_2 film when it is annealed at 70 °C. The change in the optical constant is due to a structural transition of VO_2 from a monoclinic to a tetragonal structure.[31] Similarly, the optical constants of GST increase after annealing at 180 °C [Fig. 1(b)]. This is a result of the structural phase transition from the amorphous state to the Face Centered Cubic (FCC) state. Since the optical constants for both VO_2 and GST change at two different temperatures, 70 °C and 180 °C, respectively, the two different films can be combined to design a composite material with multiple effective refractive indices and corresponding reflective states.

a)Authors to whom correspondence should be addressed: LongYi@ntu.edu.sg and robert_simpson@sutd.edu.sg

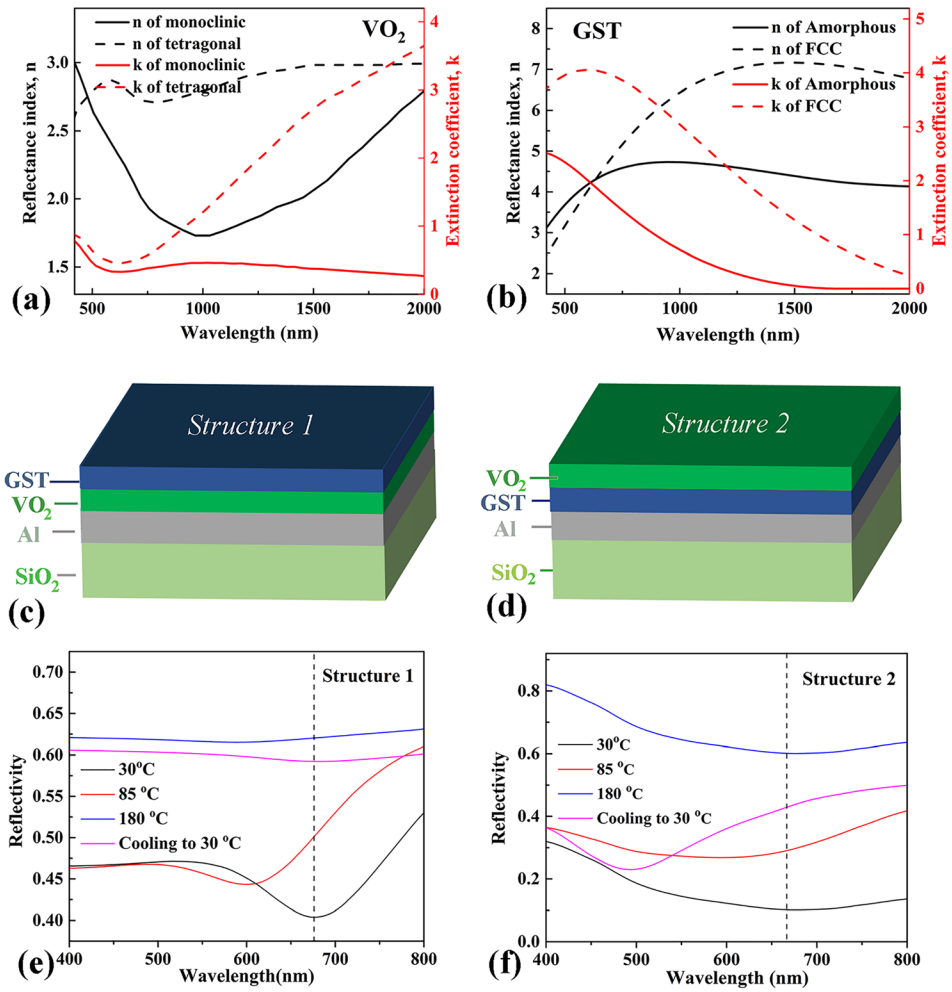

FIG. 1. Optical constant n and k of (a) VO_2 in monoclinic and tetragonal states; (b) GST in amorphous and Face Centered Cubic (FCC) states. Schematic of the nanostructures: (c) GST/VO_2/Al/Substrate (Structure 1); (d) VO_2/GST/Al/Substrate (Structure 2); (e) GST (100 nm)/VO_2 (50 nm)/Al (100 nm)/SiO_2 (Structure 1) and VO_2 (20 nm)/GST (20 nm)/Al (100 nm)/SiO_2 (Structure 2).

The nanostructure layer order has two possibilities: (1) The VO_2 layer is sandwiched between GST and Al layers, which we call "Structure 1," and (2) the GST layer is sandwiched between VO_2 and Al layers, which we call "Structure 2." Schematic diagrams of the possible nanolayer designs are shown in Figs. 1(c) and 1(d). We modeled the reflectivity of these two possible nanostructures at different temperatures, and the results are shown in Figs. 1(e) and 1(f). We found that four different reflective states could be achieved for both structures. However, the reflectivity contrast between the four states is greater for Structure 2. As can be seen in Fig. 1, the maximum change in reflectivity is 48% for Structure 2 and just 21% for Structure 1. Hence, we chose the SiO_2/Al/GST/VO_2 (Structure 2) for further optimization.

Figure 2 shows that the reflectivity of Structure 2 is strongly dependent on the phase change material layer thickness. Therefore, the transfer matrix method was used to model Fresnel's equations for reflection from stacked thin films. This model was then used to optimize the VO_2 and GST layers. The layers' thicknesses were gradually increased from 10 nm to 80 nm with a step of 10 nm. The corresponding reflectivity, VO_2 thickness, and GST thickness matrices are plotted in Figs. 2(a)–2(d). The color indicates the reflectivity of the nanostructure for a particular layer thickness of VO_2 and GST. We can see that at room temperature, the 60 nm GST and 10 nm thick VO_2 structure exhibits the maximum reflectivity. Increasing the structure's temperature to 70 °C increases the reflectivity for the thicker GST and thinner VO_2 layers. In contrast, the reflectivity decreases for the thicker GST and VO_2 layers at 190 °C, see Figs. 2(b) and 2(c). Upon subsequent cooling to room temperature, the reflectivity increases for the thicker layers and the reflectivity is minimized for an intermediate layer thickness of 40–60 nm, see Fig. 2(d). These results show that two different thicknesses of VO_2, 70 nm and 80 nm, in combination with a 50 nm layer of GST give four distinct optical levels, as shown in Figs. 2(e) and 2(f). Since the structure with a 70 nm thick layer of VO_2 has a greater optical contrast than the 80 nm thick VO_2 layer, the 70 nm thick VO_2 structure was chosen for fabrication and characterization.

The VO_2 layer was fabricated on a silica substrate using the solution-based method[32] at 550 °C, and the GST layer was deposited by radio-frequency (RF) sputtering a 99.99% pure 50 nm diameter GST alloy target at 30 W. First, the VO_2 layer of 70 nm was deposited, and then, a 50 nm thick GST layer was sputtered followed by a 100 nm Al reflective layer, which was deposited from a second target at 100 W. The Al top layer acts as a mirror to enhance the reflected signal during the measurement. This structure is designed for reflectivity measurements through the substrate, see Fig. 3(a). We chose this design such that the VO_2 layer could be deposited before the GST, because the VO_2 synthesis is performed at 550 °C. At this temperature, the GST layer would crystallize during fabrication. The GST and Al sputter

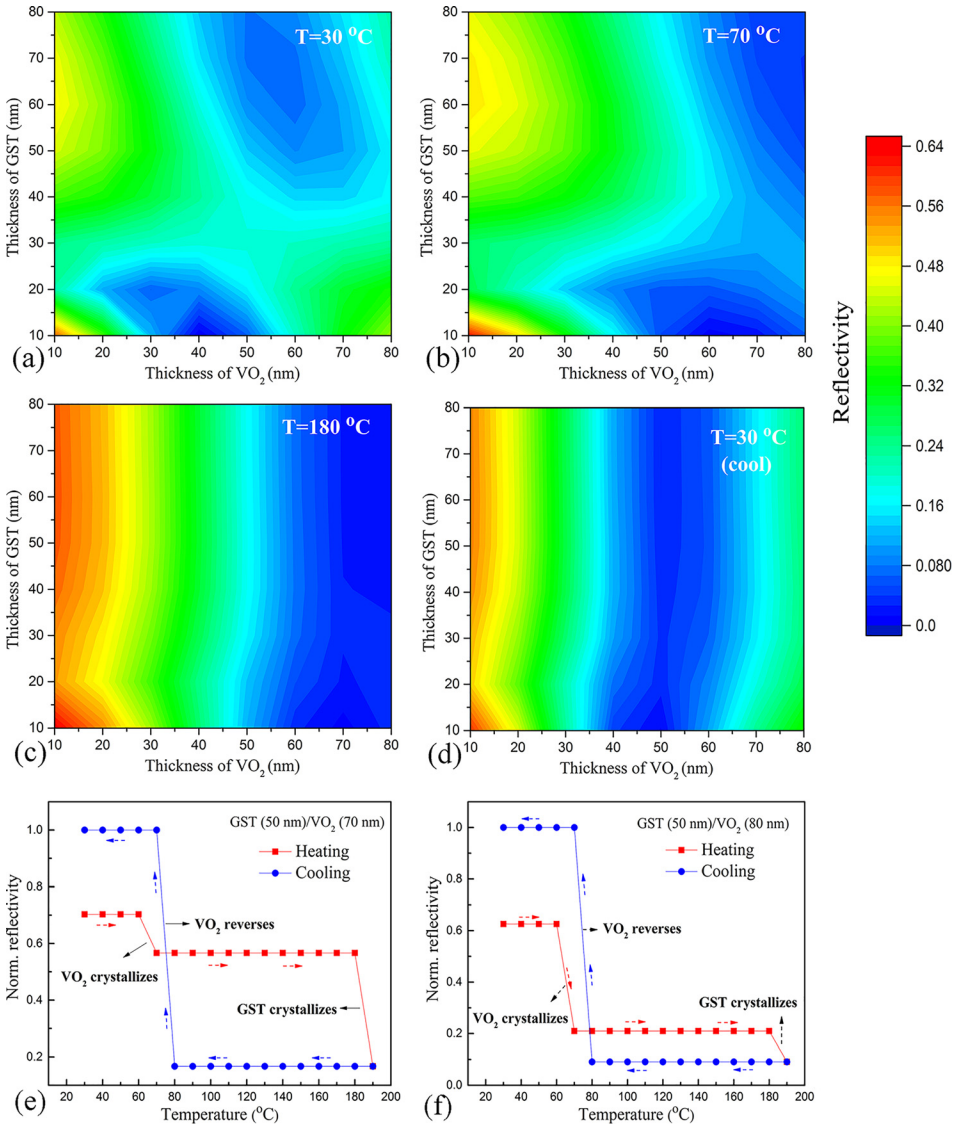

FIG. 2. The reflectivity of Structure 2 (SiO_2/GST/VO_2/Al) is simulated at a wavelength of 680 nm at a temperature of (a) 30 °C, (b) 70 °C, (c) 180 °C, and (d) after cooling to 30 °C. The reflectivity change with temperature based on (e) SiO_2/Al (100 nm)/GST (50 nm)/VO_2 (70 nm) and (f) SiO_2/Al (100 nm)/GST (50 nm)/VO_2 (80 nm) nanostructures.

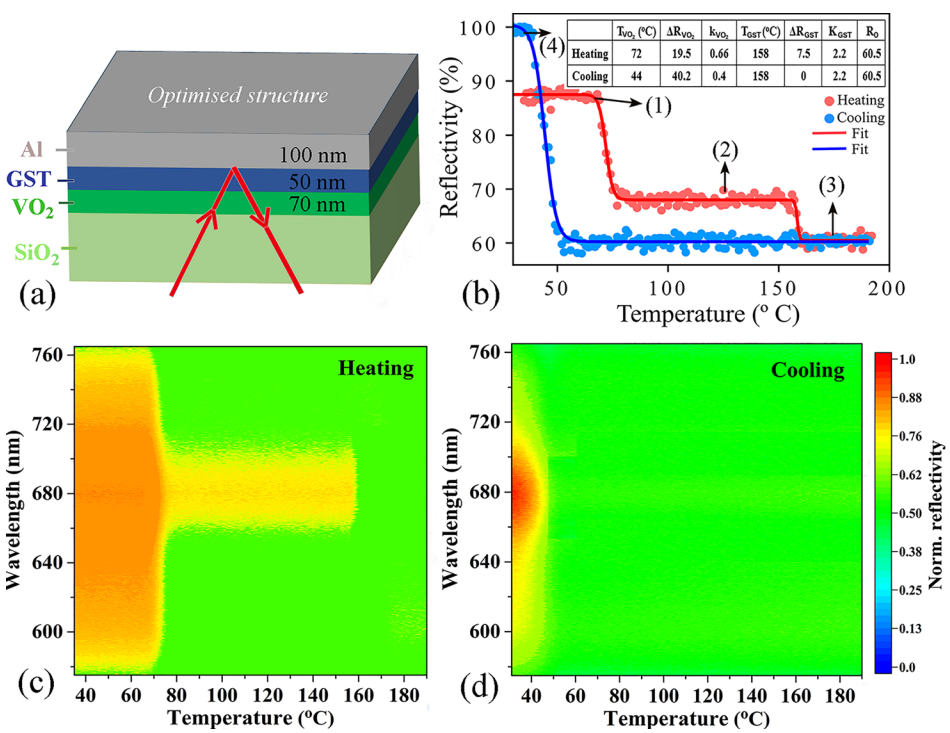

	T_{VO_2} (°C)	ΔR_{VO_2}	k_{VO_2}	T_{GST} (°C)	ΔR_{GST}	K_{GST}	R_0
Heating	72	19.5	0.66	158	7.5	2.2	60.5
Cooling	44	40.2	0.4	158	0	2.2	60.5

FIG. 3. Measured reflectivity as a function of temperature. (a) The sample schematic and reflectivity measurement arrangement through the substrate. (b) Average reflectivity across the 660 to 700 nm spectral band as a function of temperature. The inset table is the fit parameters. Reflectivity spectrum as a function of temperature during (c) heating and (d) cooling.

deposition process was carried out at a pressure of 0.5 Pa in the pure argon atmosphere. In all cases, the vacuum chamber pressure was better than 2.7×10^{-5} Pa. The reflectivity of the nanostructures was measured in the visible spectrum using spectrometer coupled to an optical microscope. A microscope furnace was used to heat the sample at 5 °C/min for the temperature dependent reflectivity measurement.

The reflectivity of the 70 nm VO_2–50 nm GST structure was measured as a function of annealing temperature to confirm the predicted multi-level optical switching ability. The VO_2 and GST layers crystallize independently at two different temperatures, as is clear in Fig. 3(b). Since the crystal fraction as a function of temperature can be described by a logistic function,[33] we analyzed the measured reflectivity versus temperature data by fitting a double logistic function

$$R = \frac{\Delta R_{VO_2}}{1 + \exp\left(k_{VO_2}(T - T_{VO_2})\right)} + \frac{\Delta R_{GST}}{1 + \exp\left(k_{GST}(T - T_{GST})\right)} + R_0,$$

where R is the reflectivity of the structure, ΔR_{VO_2} is the change reflectivity due to the VO_2 phase transition at temperature T_{VO_2}, which occurs at a rate of k_{VO_2}, and ΔR_{GST} is the change reflectivity due to the GST phase transition at temperature T_{GST}, which occurs at a rate of k_{GST}. R_0 is the minimum reflectivity of the structure, which occurs when both layers have crystallized. The fit parameters are shown in the inset table of Fig. 3(b).

Figures 3(c) and 3(d) show the reflectivity spectra as a function of temperature. The reflectivity was normalized against an Al mirror to estimate the absolute reflectivity. Initially, at room temperature, we see that the structure is 87% reflective. This is the first reflective state, denoted as (1) in Fig. 3(b). Then, the reflectivity decreases at 72 °C, indicating the metal-to-insulator transition of the VO_2 layer, thus producing the second reflective state, denoted as (2) in Fig. 3(b). Further increasing the temperature causes the GST layer to undergo a structural phase transition at 158 °C, thus decreasing the overall reflectivity to the third reflective state, denoted as (3) in Fig. 3(b). Cooling from 200 °C causes the reflectivity to increase at 44 °C, due to the VO_2 reversible transition back to an insulator. This results in the fourth reflective state, denoted as (4) in Fig. 3(b). The reflectivity changes at 44 °C, 72 °C, and 158 °C are in good agreement with our simulated reflectivity versus temperature result for Structure 2, which is shown in Fig. 2(f). Structure 2 was designed to exhibit strong reflectivity changes at a wavelength of 680 nm; however, at different wavelengths, the four states can have a similar low reflectivity. This means that a pump laser wavelength that is highly absorbed in all four states can be used to switch the reflectivity at the probe wavelength of 680 nm.

The average reflectivity across the spectral range from 660 to 700 nm is shown in Fig. 3(b). It shows that the crystallization temperature of VO_2 is $T_{VO2} = 72$ °C and the crystallization temperature of GST is $T_{GST} = 158$ °C. These transitions are very close to the crystallization temperature of the individual VO_2 and GST thin films. This is important because it shows that the GST crystallization temperature is not influenced by the VO_2 phase transition, i.e., VO_2 does not seem to seed crystallization of GST, which is sometimes seen in related materials.[34] We were initially worried that the stability of the solution deposited VO_2 layer and the possibility of Ge atoms from the GST layer reacting with oxygen atoms in the VO_2 layer. If this had happened, we would have expected the GST crystallization temperature to increase.[35] However, the GST crystallization temperature is 158 °C which is the same as the isolated GST film. This implies that the Ge atoms are unoxidized. Upon cooling, there is only one transition, which occurs at $T_{VO_2} = 44$ °C, because the GST layer remains in its metastable, FCC phase. The absolute change in reflectivity is 44%, which corresponds to a 1.65 factor increase in the reflected intensity. The GST layer, however, appears to crystallise more abruptly than VO_2. Indeed, the reflectivity of the structure is almost twice as sensitive to a unit temperature change at 158 °C compared to 72 °C and 44 °C. As both GST and VO_2 show a high endurance to phase change cycling, we also expect phase change switching in this 2-bit layer to exhibit a high cycle endurance. The cycle endurance will be properly characterized in our future work.

We have designed, demonstrated, and characterized a 2-bit, 4-state phase change optical switch that employs two different phase change materials: VO_2 and GST. The matrix transfer method was used to maximize the reflectivity dynamic range. We can easily imagine how adding other PCMs with different optical constants and transition temperatures can further increase the bit-depth of this type of design. Four different optical states were achieved with an overall optical contrast of 44%, which is in reasonable agreement with the simulated result. This type of multilevel switch opens further possibilities to design active photonic devices with multi-bit functionality. In particular, we foresee these structures being combined with metamaterials that can be tuned to multiple resonant frequencies.

This research was performed under the auspices of the SUTD-MIT International design center (IDC) and funded by the A-Star Singapore-China Joint Research Program (Grant No. 1420200046). Y. Ke and Y. Long acknowledge the funding support from the National Research Foundation, Prime Ministers Office, Singapore, under its Campus of Research Excellence and Technological Enterprise (CREATE) programme, Ministry of Education (MOE) Tier one, RG124/16. Y. Meng is grateful to the China Scholarship Council (CSC) for funding his research experience at SUTD.

[1]H. Yu, K. Lee, J. Park, and Y. K. Park, Nat. Photonics. **11**(3), 186 (2017).
[2]M. Wuttig, H. Bhaskaran, and T. Taubner, Nat. Photonics **11**, 465–476 (2017).
[3]S. Wu, M. Chen, M. T. Barako, V. Jankovic, P. W. C. Hon, L. A. Sweatlock, and M. L. Povinelli, Optica **4**(11), 1390–1396 (2017).
[4]Y. Shen, N. C. Harris, S. Skirlo, M. Prabhu, T. Baehr-Jones, M. Hochberg, X. Sun, S. Zhao, H. Larochelle, D. Englund *et al.*, Nat. Photonics. **11**(7), 441 (2017).
[5]Z. L. Sámson, K. F. MacDonald, F. De Angelis, B. Gholipour, K. Knight, C. C. Huang, E. Di Fabrizio, D. W. Hewak, and N. I. Zheludev, Appl. Phys. Lett. **96**, 143105 (2010).
[6]K. F. MacDonald, Z. L. Samson, M. I. Stockman, and N. I. Zheludev, Nat. Photonics **3**(1), 55–58 (2009).

[7]C. D. Wright, P. Hosseini, and J. A. V. Diosdado, Adv. Funct. Mater. **23**, 2248–2254 (2013).
[8]M. Rudé, J. Pello, R. E. Simpson, J. Osmond, G. Roelkens, J. J. G. M. van der Tol, and V. Pruneri, Appl. Phys. Lett. **103**(14), 141119 (2013).
[9]M. Rude, R. E. Simpson, R. Quidant, V. Pruneri, and J. Renger, ACS Photonics **2**(6), 669–674 (2015).
[10]T. Cao, C. Wei, R. E. Simpson, L. Zhang, and M. J. Cryan, Sci. Rep. **4**, 3955 (2014).
[11]W. Dong, Y. Qiu, X. Zhou, A. Banas, K. Banas, M. B. H. Breese, T. Cao, and R. E. Simpson, Adv. Opt. Mater. **6**, 1701346 (2018).
[12]J. Y. Suh, E. U. Donev, D. W. Ferrara, K. A. Tetz, L. C. Feldman, and R. F. Haglund, Jr., J. Opt. A: Pure Appl. Opt. **10**(5), 055202 (2008).
[13]Z. Zhu, P. G. Evans, R. F. Haglund, and J. Valentine, Nano Lett. **17**(8), 4881–4885 (2017).
[14]T. Hira, T. Homma, T. Uchiyama, K. Kuwamura, and T. Saiki, Appl. Phys. Lett. **1039**, 241101 (2013).
[15]K. Shportko, S. Kremers, M. Woda, D. Lencer, J. Robertson, and M. Wuttig, Nat. Mater. **7**(7), 653–658 (2008).
[16]J. K. Behera, X. Zhou, J. Tominaga, and R. E. Simpson, Opt. Mater. Express **7**(10), 3741–3759 (2017).
[17]M. Wuttig and N. Yamada, Nat. Mater. **6**(11), 824–832 (2007).
[18]A. Holsteen, I. S. Kim, and L. J. Lauhon, Nano Lett. **14**, 1898–1902 (2014).
[19]T. Yajima, T. Nishimura, and A. Toriumi, Nat. Commun. **6**, 10104 (2015).
[20]P. Li, X. Yang, T. W. Maß, J. Hanss, M. Lewin, A. K. U. Michel, M. Wuttig, and T. Taubner, Nat. Mater. **15**, 870–875 (2016).
[21]D. Ji, Y. Wang, L. Chi, and H. Fuchs, Adv. Funct. Mater. **25**, 3855–3859 (2015).
[22]N. Mahmood, C. Z. Zhang, F. Liu, J. H. Zhu, and Y. L. Hou, ACS Nano **7**, 10307 (2013).
[23]D. Chao, C. Zhu, X. Xia, J. Liu, X. Zhang, J. Wang, P. Liang, J. Lin, H. Zhang, Z. Shen, and H. Fan, Nano Lett. **15**, 565–573 (2015).
[24]K. Fan and W. J. Padilla, Mater. Today **18**(1), 39–50 (2015).
[25]H. N. Krishnamoorthy, Y. Zhou, S. Ramanathan, E. Narimanov, and V. M. Menon, Appl. Phys. Lett. **104**(12), 121101 (2014).
[26]H. Lim, N. Stavrias, B. C. Johnson, R. E. Marvel, R. F. Haglund, and J. C. McCallum, J. Appl. Phys. **115**, 093107 (2014).
[27]Y. Meng, J. K. Behera, S. Wen, R. E. Simpson, J. Shi, L. Wu, Z. Song, J. Wei, and Y. Wang, Adv. Opt. Mater. **6**, 1800360 (2018).
[28]S. Larouche and L. Martinu, Appl. Opt. **47**(13), C219–C230 (2008).
[29]G. E. Jellison and F. A. Modine, Appl. Phys. Lett. **69**, 371–373 (1996).
[30]L. T. Chew, W. Dong, L. Liu, X. Zhou, J. Behera, H. Liu, and R. E. Simpson, Proc. SPIE **10345**, 103451B (2017).
[31]S. Milošević, I. Stojković, S. Kurko, J. G. Novaković, and N. Cvjetićanin, Ceram. Int. **38**(3), 2313–2317 (2012).
[32]Y. Ke, X. Wen, D. Zhao, R. Che, Q. Xiong, and Y. Long, ACS Nano **11**(7), 7542–7551 (2017).
[33]I. Avramov and J. Šesták, J. Therm. Anal. Calorim. **118**(3), 1715–1720 (2014).
[34]R. E. Simpson, P. Fons, A. V. Kolobov, M. Krbal, and J. Tominaga, App. Phys. Lett. **100**(2), 021911 (2012).
[35]X. Zhou, Y. Du, J. K. Behera, L. Wu, Z. Song, and R. E. Simpson, ACS Appl. Mater. Interfaces **8**(31), 20185–20191 (2016).